ISSN No:-2456-2165 https://doi.org/10.38124/ijisrt/26nov1141

Deposition Temperature-Driven Evolution of Manganese Ferrite Thin Films: Structural, Optical, Morphological, Electrical and Electrochemical Investigations

V. B. Zadke[1]; Dr. R. V. Suryawanshi[2]; Dr. M. A. Barote[3]; R. U. Shelke[1]; Dr. M. B. Awale[1]; Dr. S. D. Lokhande[1]; Dr. M. B. Kumbhar[1]

[1]Thin Film and Materials Science Research Laboratory, Department of Physics, Dayanand Science College, Latur-413512, M.S., India
[2]Department of Electronics, Azad Mahavidyalaya, Ausa, Ta. Ausa, Dist. Latur-413520, M.S., India
[3]Department of Physics, Azad Mahavidyalaya, Ausa, Ta. Ausa, Dist. Latur-413520, M.S., India

Publication Date: 2026/11/27

Abstract: Manganese ferrite ($MnFe_2O_4$) thin films were synthesised by chemical spray pyrolysis at different deposition temperatures to assess structural, optical, morphological, and electrochemical properties for supercapacitor applications. X-ray diffraction confirmed a cubic spinel structure, with the largest crystallite size (36.32 nm) at 375ºC. Field-emission scanning electron microscopy revealed nanogranular morphology. UV–Visible spectroscopy showed a temperature-dependent band gap, reaching a minimum of 2.68 eV at 375 °C. The resistivity measurements confirmed semiconducting behaviour. The film prepared at 375ºC attained the highest specific capacitance of 333.48 F g^{-1} and retained 85.27% of its capacitance after 5,000 cycles at 1 mA cm^{-2} and 4 mA cm^{-2} current densities, respectively. Electrochemical impedance spectroscopy exhibited the lowest series resistance and charge-transfer resistance for this film (9.456 and 170.6 Ω, respectively). These results show that deposition temperature influences the $MnFe_2O_4$ film properties, with the film deposited at 375 °C exhibiting promising electrochemical performance for supercapacitor applications.

How to Cite: V. B. Zadke; Dr. R. V. Suryawanshi; Dr. M. A. Barote; R. U. Shelke; Dr. M. B. Awale; Dr. S. D. Lokhande; Dr. M. B. Kumbhar (2026) Deposition Temperature-Driven Evolution of Manganese Ferrite Thin Films: Structural, Optical, Morphological, Electrical and Electrochemical Investigations. *International Journal of Innovative Science and Research Technology,* 11(11), 1971-1984. https://doi.org/10.38124/ijisrt/26nov1141

I. INTRODUCTION

The demand for electrical energy continues to increase, which makes its efficient utilisation and storage of utmost importance. Conventionally, batteries and capacitors have been used to store and deliver electrical energy. However, renewable energy systems require storage devices with simultaneous high power density and high energy density, which is a major area of current research [1]. Batteries have high energy density, i.e. they can store more total energy per unit mass or volume than capacitors. But their stored energy delivery is slower than capacitors, i.e. they possess lower power density [2]. This has led to extensive research being directed to alternative energy storage technologies with higher efficiency, better electrochemical performance and affordability [3]. One of the most promising devices for energy storage is electrochemical supercapacitors (SCs), with characteristics that lie between those of conventional capacitors and batteries. Supercapacitors have several favourable features, including high power-handling capacity, high current capability, excellent cycling stability, fast charge-discharge rates, long cycle life, and a wide operating temperature range. Furthermore, they are relatively lightweight, economical and eco-friendly, and require minimal maintenance [1], [4], [5], [6]. These features make SCs favourable for applications in electric vehicles, portable electronic devices, power backup, memory backups, etc. [1], [7], [8].

Supercapacitors can be categorized into three types based on their charge storage mechanism. Electrochemical double-layer capacitors (EDLCs) store charge physically through reversible ion adsorption and desorption at the electrode-electrolyte interface. In pseudocapacitors, faradaic mechanisms are responsible for energy storage at or near the surface of electrodes. Hybrid supercapacitors use both types of charge storage mechanisms [6], [9], [10], [11]. Pseudocapacitors can attain higher specific capacitance and energy density compared to EDLCs due to the involvement of fast faradaic redox processes [12], [13]. Metal oxides and

ISSN No:-2456-2165 https://doi.org/10.38124/ijisrt/26nov1141

conducting polymers are the electrode materials used in pseudocapacitors [13]. Among the various factors affecting supercapacitor performance, the electrode material plays a very crucial role in determining the specific capacitance and charge storage, which are strongly influenced by its morphology and structure [4], [14]. Of the many electrode materials investigated for pseudocapacitors, transition metal oxides like spinel ferrites have attracted considerable attention [15]. They have the general formula MFe_2O_4 (M = Co, Ni, Mn, Cu, Zn), having a cubic structure, in which oxygen anions form a closely packed lattice and metal cations occupy tetrahedral (A) or octahedral (B) sites [7], [16].

Among spinel ferrites, manganese ferrite ($MnFe_2O_4$, MFO) is a potential electrode material for supercapacitors because of its chemical stability, high specific capacitance and excellent cycling stability. It is abundantly available, ecologically safe, and easy to synthesise [16], [17], [18], [19]. Many previous studies have exhibited the potential of MFO in electrochemical energy storage and have explored its preparation in thin-film form using different deposition techniques. In particular, Zate et al. (2016) reported the synthesis of $MnFe_2O_4$ thin films on glass and stainless-steel substrates using the chemical spray pyrolysis technique at 400 °C. They confirmed the formation of the spinel phase with nodule-type morphology. The maximum specific capacitance value obtained was 313 F g^{-1} at a scan rate of 5 mV s^{-1} and 293.5 F g^{-1} at a current density of 1 mA cm^{-2} using cyclic voltammetry (CV) and galvanostatic charge-discharge (GCD), respectively, for 1 M KOH electrolyte [18]. Bhosale R. P. et al. (2024) prepared manganese ferrite thin films by electrodeposition and explored the effect of deposition time on film morphology and electrochemical properties. They observed that the best results were obtained for the films with worm-like morphology, attaining a specific capacitance of 227 F g^{-1} at a current density of 2 A g^{-1}, specific energy of 35.1 Wh kg^{-1}, specific power of 3.1 kW kg^{-1} and capacitive retention of 89.3 % after 5000 cycles [19]. Giribaldi A. et al. (2026) studied the influence of deposition temperature on the properties of $MnFe_2O_4$ thin films deposited on silica substrates using the pulsed laser deposition technique and concluded that their crystallinity was observed to increase with rising deposition temperature [20].

Spray pyrolysis is a relatively simple, low-cost thin film deposition technique that allows easy adjustment of deposition parameters to control film properties. It is suitable for the synthesis of spinel metal oxides like manganese ferrite for a variety of applications. Parameters such as spray rate, precursor solution concentration and quantity, nozzle-to-substrate distance, deposition temperature, etc., influence the properties of the films [21]. Among these, deposition temperature plays an essential role in determining the growth, crystallinity, morphology and properties of the films, which can be modified and controlled by varying the deposition temperature [22]. Understanding these variations helps in assessing their suitability for different technological applications. In the present study, the manganese ferrite thin films were synthesised using spray pyrolysis on both amorphous glass and FTO-coated glass substrates at five different deposition temperatures (325, 350, 375, 400 and 425 °C). The films deposited on amorphous glass substrates were investigated for their structural, morphological, elemental, optical and electrical properties, whereas those deposited on FTO-coated glass were used for electrochemical characterisation studies such as CV, GCD and electrochemical impedance spectroscopy (EIS). The influence of deposition temperature on the physicochemical characteristics and electrochemical charge-storage behaviour of the prepared films was thus investigated to establish the relationship between deposition conditions, film properties and electrochemical performance.

II. EXPERIMENTAL DETAILS

$MnFe_2O_4$ thin films were prepared using the chemical spray pyrolysis technique on ultrasonically cleaned amorphous glass and FTO-coated glass substrates (resistivity below 7 Ω cm^2). The synthesis was carried out using Manganese (II) Nitrate Hexahydrate [$Mn(NO_3)_2.6H_2O$] and Ferric Nitrate Nonahydrate [$Fe(NO_3)_3.9H_2O$] as precursor solutions. The chemicals used were AR grade and obtained from Sigma-Aldrich and Himedia, respectively. Double-distilled water and Ethanol were used as solvents. For each deposition, 5 ml of Manganese Nitrate of 0.20 M and 10 ml of ferric nitrate 0.20 M were separately dissolved in double-distilled water and then mixed thoroughly by stirring for 20 min. 5 ml ethanol was added to this solution before deposition. A total of 20 ml solution was thus sprayed onto preheated substrates. The films were fabricated at five different deposition temperatures: 325, 350, 375, 400 and 425 ºC. Other preparative parameters such as a spray rate of 2 ml min^{-1}, nozzle-to-substrate distance of 28 cm, and a spray pressure of 0.30 MPa were kept constant for each deposition. Compressed air was utilised as a carrier gas to atomise the spray. A thermocouple connected to the surface of the hot plate helped to keep the deposition temperature under control within ±5°C. During each deposition, 3 samples of $MnFe_2O_4$ thin films on amorphous glass substrates (7.5 cm x 2.5 cm x 0.135 cm) and 1 sample of $MnFe_2O_4$ on FTO substrates (1cm x 1cm) were obtained.

➢ *Characterisation:*

The Structural properties of the $MnFe_2O_4$ thin films were studied using an X-ray diffractometer (PW-3710) with Cu-kα radiation (λ= 1.5406 Å). Field-effect scanning electron microscopy (FESEM) (Model No. FEI Nova Nano SEM 450) was used to study the surface morphology of the films**.** Elemental and compositional analysis was done using energy-dispersive X-ray analysis (EDAX). A UV-Vis spectrophotometer (SHIMADZU-1700) was used to obtain the optical absorption spectra and determine the optical bandgap of the manganese ferrite thin films in the wavelength range of 200 to 1100 nm. The direct current (DC) two-point probe method was used to determine the electrical resistivity of the thin films. Electrochemical measurements of the $MnFe_2O_4$ thin films were performed using an electrochemical analyser (CH Instruments, Auto Lab). The standard three-electrode cell configuration was used with 1 M KOH as the electrolyte, 1cm^2 $MnFe_2O_4$ thin films as the working electrode, platinum (Pt) wire as the counter electrode and Ag/AgCl as the reference electrode. Cyclic Voltammetry

ISSN No:-2456-2165 https://doi.org/10.38124/ijisrt/26nov1141

(CV), Galvanostatic Charge-Discharge (GCD) and Electrochemical Impedance Spectroscopy (EIS) studies were carried out for the $MnFe_2O_4$ thin films to study their electrochemical performance.

III. RESULTS

➢ *Chemical Reaction:*

In the spray pyrolysis technique, the precursor solution is sprayed onto preheated substrates to obtain thin films of the desired chemical compound. The chemical reaction between Mn $(NO_3)_2$. $6H_2O$ and Fe $(NO_3)_3.9H_2O$ resulted in the formation of $MnFe_2O_4$ thin films. The MFO thin films obtained at various deposition temperatures have a light yellowish-brown to dark reddish-brown colour.

The chemical reactions involved in the formation of $MnFe_2O_4$ thin films can be represented as follows:

The manganese nitrate solution first decomposes to form manganese hydroxide as follows:

$$Mn(NO_3)_2.6H_2O + 2H_2O \longrightarrow Mn(OH)_2 + 2HNO_3 + 6H_2O \quad (1)$$

Similarly, the ferric nitrate solution forms ferric hydroxide due to decomposition as follows:

$$2Fe(NO_3)_3.9H_2O + 6H_2O \longrightarrow 2Fe(OH)_3 + 6HNO_3 + 18H_2O \quad (2)$$

In the end, the manganese hydroxide and ferric hydroxide react together and lead to the formation of manganese ferrite through the following reaction:

$$Mn(OH)_2 + 2Fe(OH)_3 \longrightarrow MnFe_2O_4 + 4H_2O \uparrow \quad (3)$$

A similar reaction mechanism is reported previously for $CoFe_2O_4$ thin films obtained by the spray pyrolysis technique [23].

➢ *Film Thickness*

Film thickness is a crucial parameter that significantly influences the properties of thin films. The gravimetric weight difference method with a sensitive microbalance (least count = 0.01mg) was used to determine the apparent film thicknesses of the spray-pyrolytically deposited $MnFe_2O_4$ thin films.

The formula to calculate thickness using this method is as follows [24].

$$t = \frac{\Delta m}{l \times b \times \rho} \quad (4)$$

Where t is the thickness of $MnFe_2O_4$ thin films, Δm is the mass difference (the difference between the weight of the film after and before deposition), l represents the length of the substrate, b is the breadth of the substrate, and ρ is the density of the material (the bulk density of $MnFe_2O_4$ is 4.77 g cm^{-3}). The estimated film thicknesses were found to be 243nm, 301nm, 454nm, 389nm, and 306nm for $MnFe_2O_4$ thin films deposited at deposition temperatures of 325°C, 350°C, 375°C, 400°C, and 425°C, respectively. Fig. 1 shows how the estimated film thickness varies with deposition temperature for spray-pyrolytically deposited $MnFe_2O_4$ thin films. The film thickness was found to increase when the deposition temperature was raised from 325°C to 375°C, and afterwards it started to decrease. The lower substrate temperatures (below 375 °C) appear insufficient for complete decomposition of the nitrate precursor solution, resulting in reduced film thickness. The highest film thickness is obtained at 375°C. However, at higher temperatures (> 375 °C), the film thickness decreases, maybe due to the changes in the deposition rate of the initial specimen. Similar behaviour has previously been reported for $NiFe_2O_4$ thin films prepared using spray pyrolysis [25].

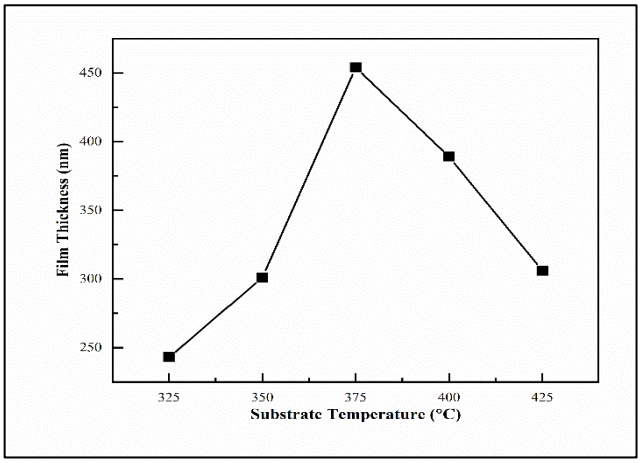


Fig 1 Variation of Film Thickness with Deposition Temperature for $MnFe_2O_4$ thin Films Deposited by the Spray Pyrolysis Technique.

➢ *Structural Analysis*

The structural properties of $MnFe_2O_4$ thin films prepared via the spray pyrolysis method on glass substrates at various deposition temperatures were studied using X-Ray diffraction (XRD) with Cu Kα radiation and 2θ in the range of 20° to 80°. Fig. 2 shows the XRD patterns of spray pyrolytically deposited $MnFe_2O_4$ thin films at deposition temperatures of 325°C, 350°C, 375°C, 400°C, and 425°C, respectively. They indicate the formation of the cubic spinel phase of $MnFe_2O_4$ with the space group Fd-3m (JCPDS card number 01-074-2403) [18]. The intense diffraction peaks were observed at 2θ values around 29.75°, 35.02°, 42.54°, 56.19°, and 61.68° with corresponding crystallographic planes (220), (311), (400), (333), and (440), respectively. Among the observed reflections, the (311) reflection exhibits the highest intensity and is characteristic of the spinel ferrite structure. No additional diffraction peaks attributable to secondary crystalline phases were observed, suggesting the formation of predominantly spinel-phase MFO thin films.

ISSN No:-2456-2165 https://doi.org/10.38124/ijisrt/26nov1141

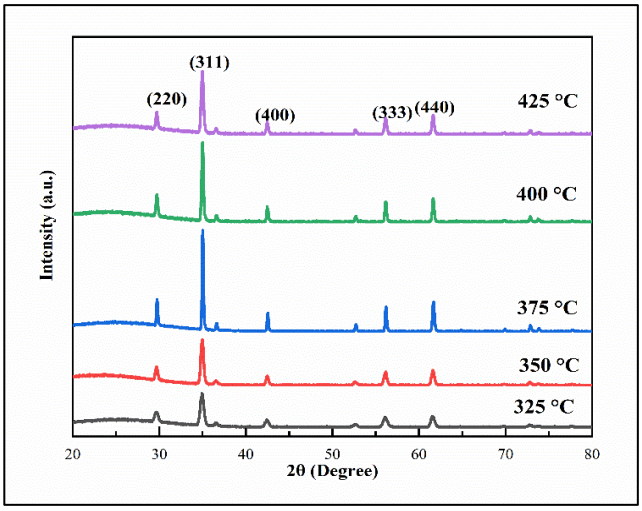


Fig 2 XRD Patterns of $MnFe_2O_4$ thin Films Deposited by the Spray Pyrolysis Technique at Different Deposition Temperatures.

Fig. 2 depicts the effect of deposition temperature on the intensity of diffraction peaks. The diffraction peak intensity increased with deposition temperature up to 375 °C and subsequently decreased. Debye-Scherrer equation was used to estimate the crystallite sizes of $MnFe_2O_4$ thin films prepared via the spray pyrolysis method at different deposition temperatures [26].

$$D = \frac{0.9\lambda}{\beta \cos\theta} \quad (5)$$

Where D is the average crystallite size, λ is the X-ray wavelength, β is the full width at half the maxima, and θ is Bragg's angle.

Table 1 Structural Parameters for $MnFe_2O_4$ thin Films Prepared by the Spray Pyrolysis Method at Different Deposition Temperatures.

Deposition temperature (°C)	2θ (°)	Observed d-spacing (Å)	Standard d-spacing (Å)	hkl	a (Å)	Crystallite Size D (nm)
325	29.6655	3.009	3.00909	220	8.510	14.38
	34.9406	2.56586	2.56616	311		
	42.4508	2.12768	2.12775	400		
	56.113	1.63774	1.63794	333		
	61.5998	1.50437	1.50455	440		
350	29.6881	3.00676	3.00909	220	8.506	20.01
	34.9601	2.56447	2.56616	311		
	42.4769	2.12643	2.12775	400		
	56.1296	1.6373	1.63794	333		
	61.618	1.50397	1.50455	440		
375	29.7527	3.00038	3.00909	220	8.494	36.32
	35.0221	2.56007	2.56616	311		
	42.5358	2.12362	2.12775	400		
	56.1925	1.63562	1.63794	333		
	61.6794	1.50262	1.50455	440		
400	29.7276	3.00286	3.00909	220	8.499	29.28
	34.998	2.56179	2.56616	311		
	42.5067	2.12501	2.12775	400		
	56.168	1.63627	1.63794	333		
	61.653	1.5032	1.50455	440		
425	29.7083	3.00477	3.00909	220	8.502	24.81
	34.9767	2.5633	2.56616	311		
	42.4896	2.12582	2.12775	400		
	56.1487	1.63679	1.63794	333		
	61.6314	1.50367	1.50455	440		

Table 1 gives the crystallite size values of $MnFe_2O_4$ thin films deposited at various deposition temperatures. The $MnFe_2O_4$ thin film deposited at 375 °C exhibited the largest crystallite size, measuring 36.32 nm. The enhanced intensity at 375 °C, together with the highest crystallite size, suggests improved crystallisation and grain growth at this deposition temperature. The crystallite sizes are comparable to those reported by Nagarajan V. et al. [27]. The lattice parameter "a" was calculated for the (311) plane using the following standard relation [28].

$$a = d\sqrt{h^2 + k^2 + l^2} \quad (6)$$

Where d is the interplanar distance and (hkl) are the Miller indices. The obtained values of the lattice parameter ranged from 8.494 to 8.510 Å and are close to the standard

ISSN No:-2456-2165 https://doi.org/10.38124/ijisrt/26nov1141

JCPDS data card value of a = 8.5110 Å (JCPDS card no. 01-074-2403) [18].

➢ *Morphological Analysis*

Fig. 3(a)–(e) presents FESEM micrographs of spray-pyrolyzed $MnFe_2O_4$ thin films deposited at different deposition temperatures. All films exhibit a continuous granular morphology with relatively uniform surface coverage and well-defined/interconnected grain boundaries [29]. At 325ºC, the surface consists of distinct, irregularly shaped grains. As the deposition temperature increases to 350 and 375 °C, the grains appear more closely packed and more coalesced, suggesting progressive densification of the film surface. The relatively compact and coalesced morphology observed at 375 °C is consistent with the enhanced crystallite growth indicated by XRD. At 400 and 425 °C, the films maintain a continuous granular structure, with comparatively finer, more uniformly distributed grains. The dense surface coverage and absence of prominent cracks suggest good film continuity and a relatively compact surface morphology.

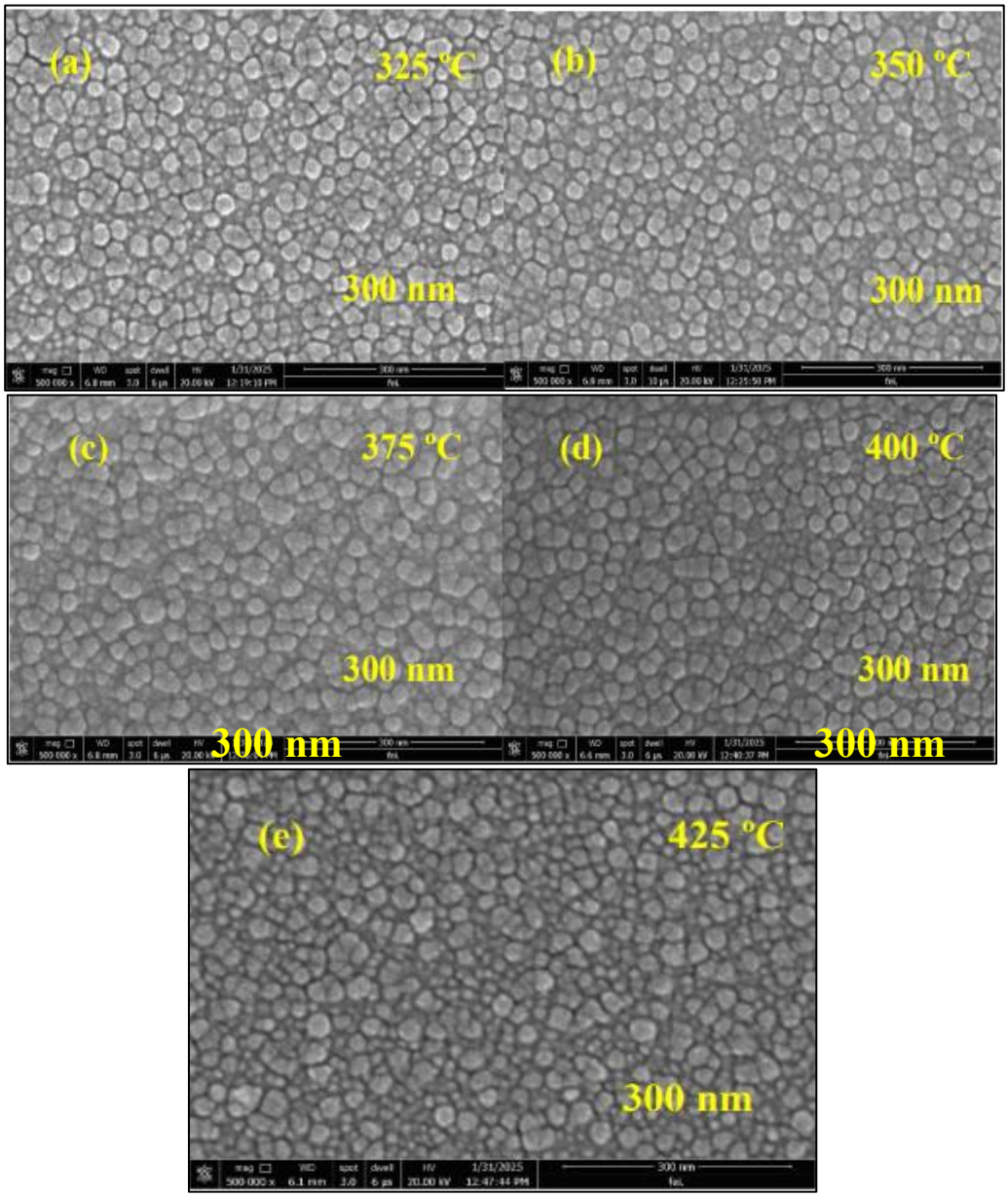


Fig 3 FESEM Micrographs of Spray-Pyrolyzed $MnFe_2O_4$ thin Films Deposited at Deposition Temperatures of (a) 325 °C, (b) 350 °C, (c) 375 °C, (d) 400 °C, and (e) 425 °C.

➢ *Compositional Analysis*

Energy-dispersive X-ray spectroscopy (EDAX) was used to evaluate the elemental composition of the prepared $MnFe_2O_4$ thin films. Fig. 4 (a) to (e) show the EDAX spectra of the $MnFe_2O_4$ thin films deposited at temperatures of 325°C to 425°C. The analysis confirmed the presence of Mn, Fe and O in the deposited films. The Mn: Fe atomic ratio remains close to the 1:2 ratio, indicating relatively consistent cation composition with increasing deposition temperature. Table 2 presents the elemental composition of the prepared MFO thin films, as determined by compositional analysis. The phase formation of cubic spinel $MnFe_2O_4$ is further supported by the XRD results discussed in Section 4.3.

ISSN No:-2456-2165 https://doi.org/10.38124/ijisrt/26nov1141

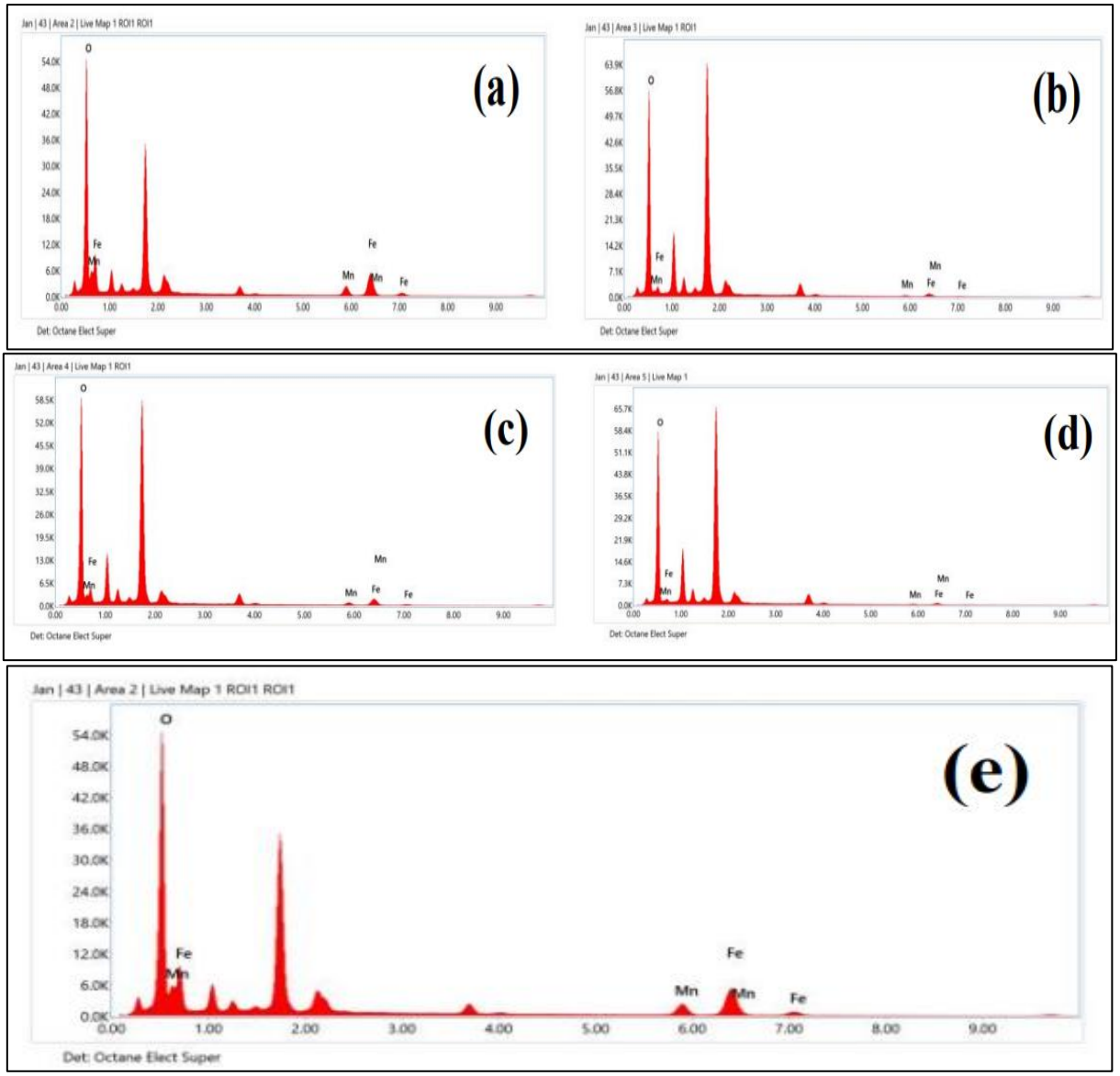


Fig 4 EDAX Spectra of Spray Pyrolyzed $MnFe_2O_4$ thin Films Prepared at Various Deposition Temperatures of (a) 325 °C, (b) 350 °C, (c) 375 °C, (d) 400 °C, and (e) 425 °C.

Table 2 Elemental Composition of Spray Pyrolyzed $MnFe_2O_4$ thin Films at Different Deposition Temperatures

Deposition temperature (℃)	Atomic Percentage of $MnFe_2O_4$ Films (%)		
	Mn	Fe	O
325	10.3	21.7	68
350	11.5	22	65.5
375	12.2	23.1	64.7
400	12	22	66
425	11.9	21.8	66.3

➢ *Optical Analysis*

The UV-Visible absorption spectra of spray pyrolysed $MnFe_2O_4$ thin films prepared by varying deposition temperature were recorded at room temperature as shown in Fig. 5(a). The bandgap energy of the $MnFe_2O_4$ thin films was determined using Tauc's relation as follows [30]:

$$\alpha = \frac{A\,(h\nu - Eg)^n}{h\nu} \quad (7)$$

Where α is the absorption coefficient, A is an energy-independent constant, E_g is the bandgap, $h\nu$ is the incident photon energy, and n = ½ or 2 for allowed direct or indirect bandgap transitions, respectively.

ISSN No:-2456-2165 https://doi.org/10.38124/ijisrt/26nov1141

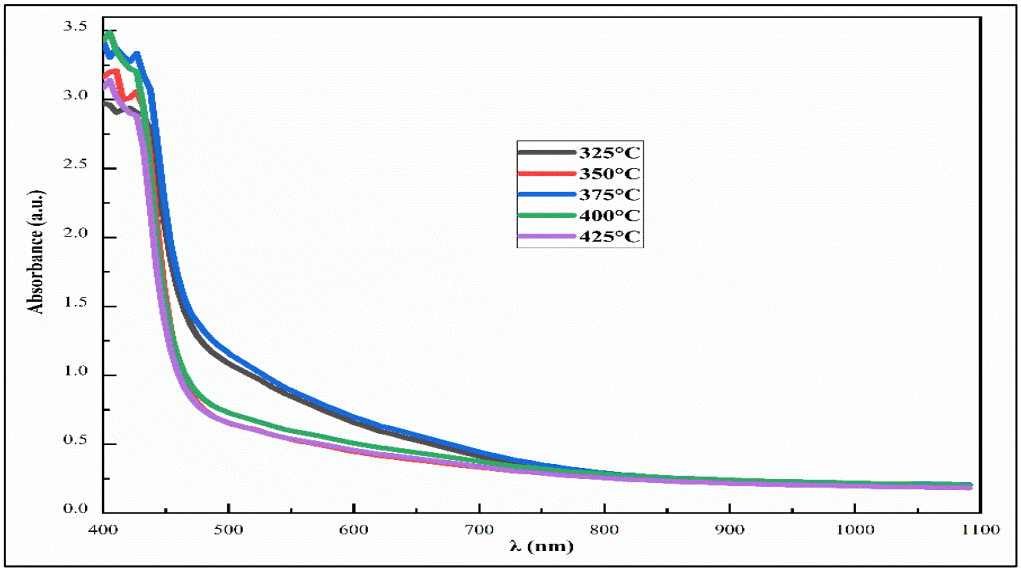


Fig 5(a) UV-Vis Absorbance Spectra of $MnFe_2O_4$ thin Films Prepared by using Spray Pyrolysis at Various Deposition Temperatures.

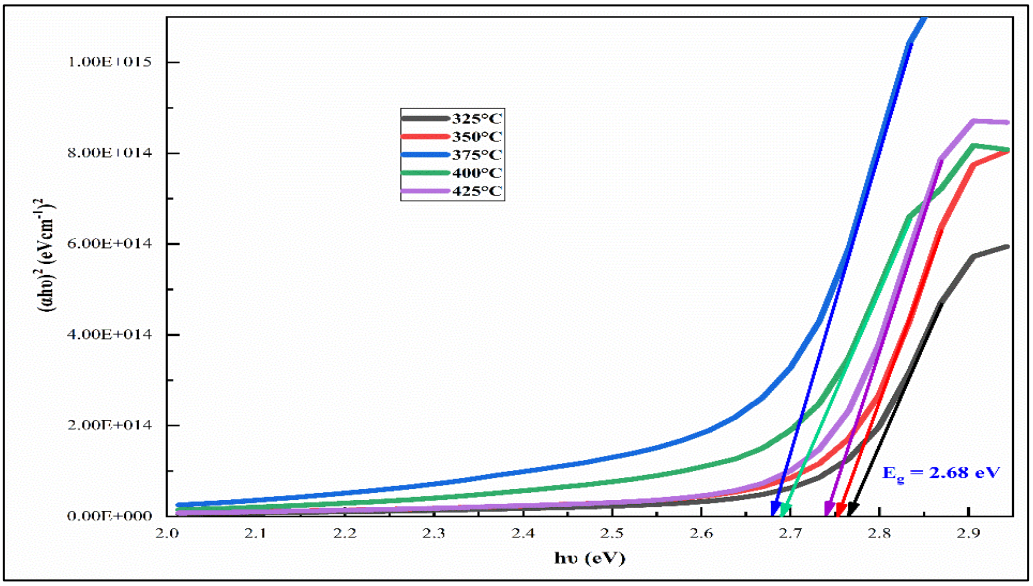


Fig 5(b) Tauc Plots of $(\alpha h\nu)^2$ Versus hν for Spray Pyrolysed $MnFe_2O_4$ thin Films Deposited at Different Temperatures.

Fig. 5(b) shows the plot of $(\alpha h\nu)^2$ versus hν for spray pyrolysed $MnFe_2O_4$ thin films prepared by varying the deposition temperature. The bandgap energy (E_g) was determined by assuming the nature of a direct allowed transition for $MnFe_2O_4$ thin films and by extrapolating the linear portion of the $(\alpha h\nu)^2$ versus hν to $(\alpha h\nu)^2 = 0$. The observed bandgap values are as given in Table 3. The estimated optical band gap of the $MnFe_2O_4$ thin films varied from 2.68 to 2.77 eV depending on the deposition temperature. The minimum optical band gap of 2.68 eV was obtained for the film deposited at 375 °C. The optical bandgap obtained in the present study is close to the range of experimentally reported values for $MnFe_2O_4$. For example, band gap values of approximately 2.59 and 2.64 eV respectively have been reported for $MnFe_2O_4$ by two studies with co-precipitation technique [31], [32], while a value of approximately 1.89 eV has been reported for spray-pyrolyzed $MnFe_2O_4$ thin films [27]. The variation in reported optical band gaps may be associated with differences in synthesis conditions, crystallite size, defect states, morphology and cation distribution.

Table 3 Energy Bandgap Values for $MnFe_2O_4$ thin Films Obtained at Various Deposition Temperatures by the Spray Pyrolysis Technique.

Sr. No.	Deposition temperature (°C)	Bandgap (eV)
1.	325	2.77
2.	350	2.75
3.	375	2.68

ISSN No:-2456-2165 https://doi.org/10.38124/ijisrt/26nov1141

4.	400	2.69
5.	425	2.73

➢ *Electrical Resistivity*

Electrical resistivity of $MnFe_2O_4$ thin films was measured under dark conditions using a DC two-point probe method over the temperature range of 300 to 500K. Figure 6 depicts the variation of the logarithm of electrical resistivity (log ρ) versus the inverse of absolute temperature (1000/T) for MFO thin films deposited using the spray pyrolysis technique at different deposition temperatures. The graph illustrates the influence of both deposition temperature and measurement temperature on the electrical transport behaviour of the prepared $MnFe_2O_4$ films.

As seen in Figure 6, the resistivity of all the deposited films decreases continuously with increasing measurement temperature, as indicated by the rise in log ρ with increasing 1000/T values. This behaviour confirms the semiconducting nature of $MnFe_2O_4$, where charge transport is largely attributed to a thermally activated conduction mechanism [33].

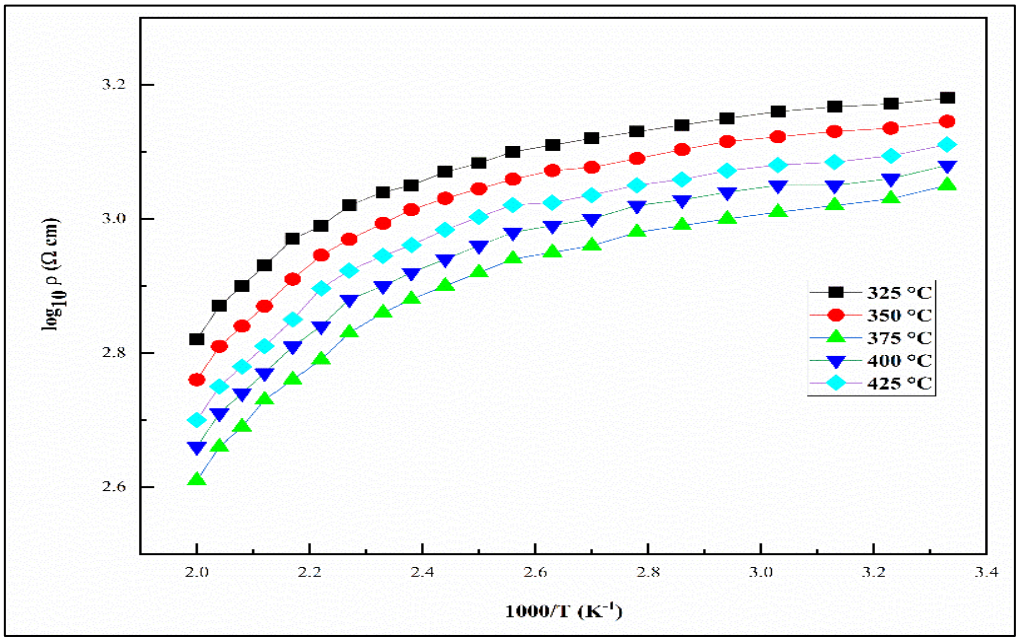


Fig 6 Variation of Log ρ with the Inverse of Absolute Temperature (1000/T) for $MnFe_2O_4$ thin Films Prepared at Various Deposition Temperatures using the Spray Pyrolysis Technique.

A comparison of the resistivity curves reveals that the deposition temperature has a significant influence on the electrical performance of the films. The sample deposited at 325 °C exhibits the highest resistivity throughout the investigated temperature range, while the resistivity decreases for the film deposited at 350 °C. The film deposited at 375 °C shows the lowest resistivity among all the samples. Improved crystallinity and larger crystallite size at 375 °C are likely responsible for the lower electrical resistivity. The films deposited at 400 and 425 °C exhibit lower resistivities than the samples prepared at 325 and 350 °C; however, their resistivities are slightly higher than those of the film deposited at 375 °C. This slight increase may be due to decreased crystallite sizes at deposition above 375 °C, leading to a decrease in carrier concentration. Table 4 shows the electrical resistivities of $MnFe_2O_4$ thin films at 300 K and 500 K. At 300 K, the minimum electrical resistivity was found to be 0.1122 × 10^4 Ω cm and 0.4074 x 10^3 Ω cm at 500 K for MFO thin films synthesized at 375 °C.

Table 4 Electrical Properties of Spray Pyrolyzed $MnFe_2O_4$ thin Films at Different Deposition Temperatures (LT; Low Temperature, HT; High Temperature)

Deposition temperature (°C)	**Electrical resistivity (Ω cm)**		**Activation energy (eV)**	
	300 K (×10^4)	**500 K (×10^3)**	**LT**	**HT**
325	0.1514	0.6607	0.0238	0.1386
350	0.1398	0.5754	0.0249	0.1371
375	0.1122	0.4074	0.0307	0.1181
400	0.1202	0.4571	0.0259	0.1301
425	0.1290	0.5012	0.0283	0.1344

ISSN No:-2456-2165 https://doi.org/10.38124/ijisrt/26nov1141

The resistivity curves display a gradual change in slope with measurement temperature. In the lower temperature region (higher 1000/T values), the resistivity changes gradually, while as the measurement temperature increases (lower 1000/T values), the slope becomes steeper, reflecting a stronger temperature dependence of resistivity. The change in slope indicates the presence of two activation energies, suggesting the possibility that different conduction mechanisms could dominate in the low- and high-temperature regions. The activation energies of spray-pyrolyzed $MnFe_2O_4$ thin films deposited at different deposition temperatures were calculated using the Arrhenius equation [28].

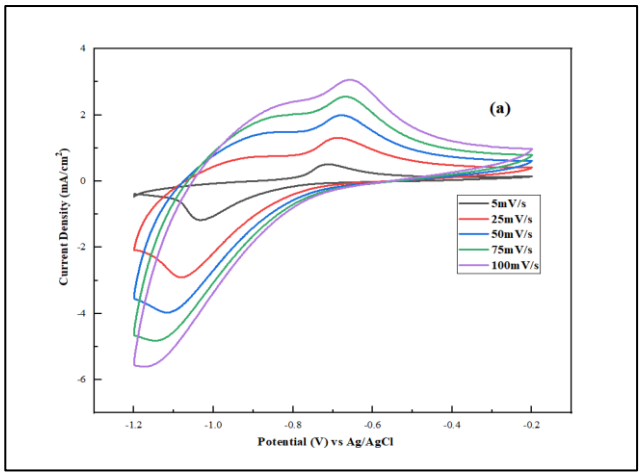
$$\rho = \rho_0 \, exp\left(\frac{E_a}{kT}\right) \quad (8)$$

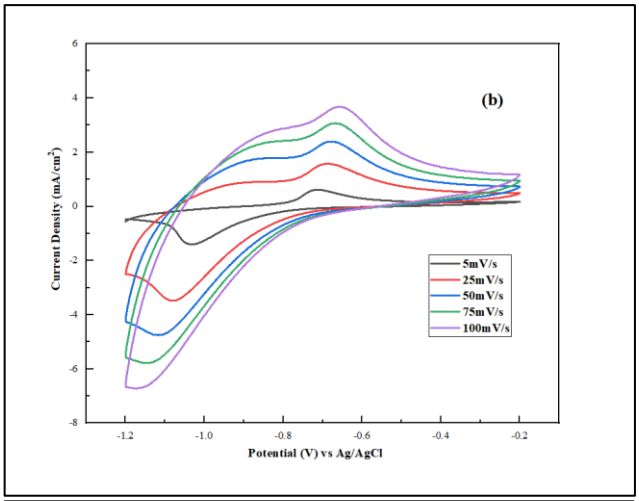
Where ρ represents the resistivity of the semiconducting material, ρ_0 stands for the resistivity constant, E_a represents activation energy, k is the Boltzmann constant, and T indicates the absolute temperature. The activation energies were determined from the slope of the plot and were found to be 0.1181–0.1386 eV and 0.0238– 0.0307 eV in the high-temperature and low-temperature regions, respectively, as mentioned in Table 4. In ferrites, electrical resistivity is influenced by the crystal structure, chemical composition, the oxidation states and concentrations of the constituent cations (including Fe^{2+} and Fe^{3+}), and their distribution between tetrahedral and octahedral sites. These features can depend on the synthesis method and conditions [28], [34].

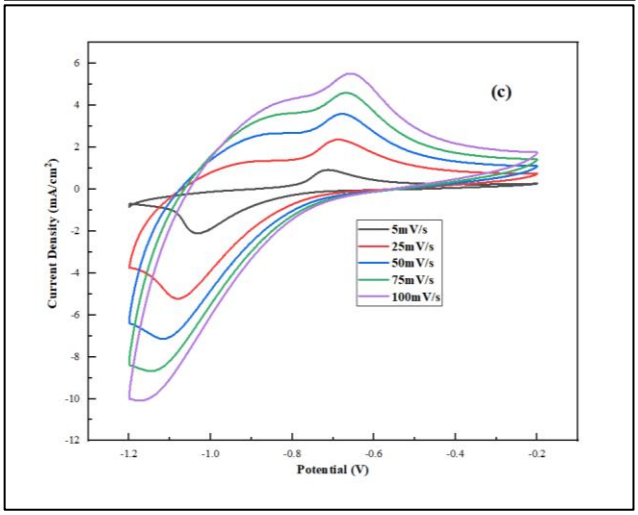
➢ *Electrochemical Characterization*

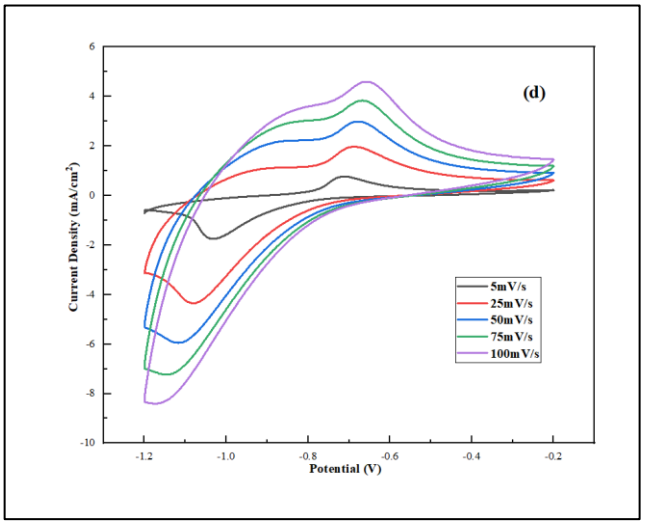
- *Cyclic Voltammetry*

Figure 7 (a – e) presents cyclic voltammograms of $MnFe_2O_4$ thin films recorded using a standard three-electrode cell configuration at different scan rates (5 mV s^{-1} to 100 mV s^{-1}) within a potential window of −1.2 to −0.2 V versus Ag/AgCl in aqueous 1 M KOH electrolyte. The presence of redox peaks in the CV curves indicates a significant faradaic contribution to the charge-storage process, suggesting pseudocapacitive behavior of the films [18]. The CV response becomes more prominent as the deposition temperature increases up to 375 °C, as evidenced by the larger enclosed CV area, then decreases for films deposited at 400 and 425 °C.









ISSN No:-2456-2165 https://doi.org/10.38124/ijisrt/26nov1141

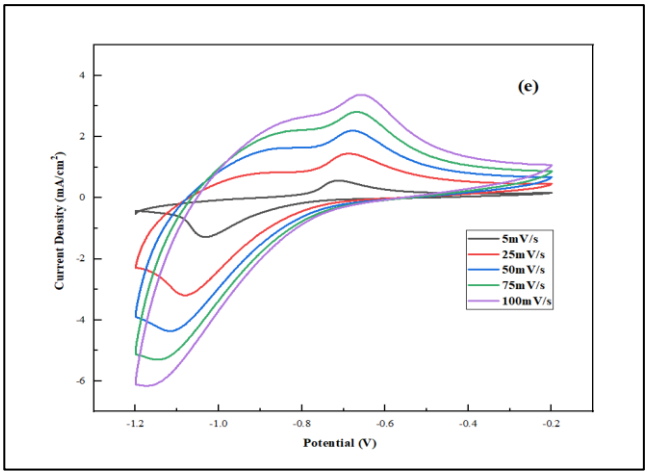
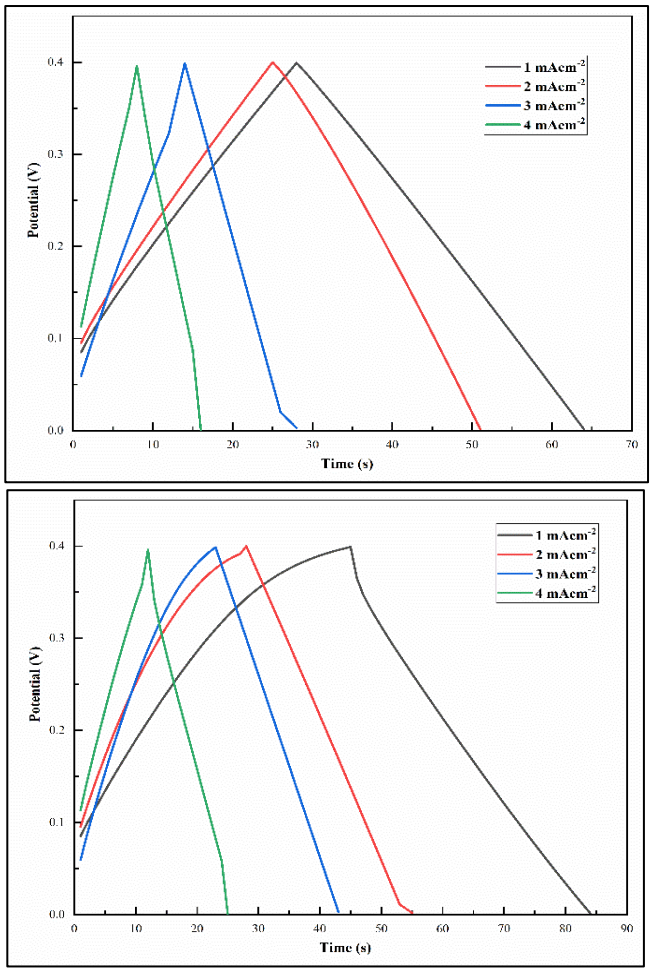


Fig 7 (a – e). Cyclic Voltammetry plots of $MnFe_2O_4$ thin Films Prepared by Spray Pyrolysis at Various Deposition Temperatures: (a) 325ºC, (b) 350ºC, (c) 375ºC, (d) 400ºC, and (e) 425ºC.

- *Galvanostatic Charge-Discharge*

Galvanostatic charge–discharge (GCD) measurements were performed at different current densities (1 mA cm^{-2} to 4 mA cm^{-2}) within the potential window range of 0 – 0.4 V using 1 M KOH electrolyte to evaluate the charge-storage behaviour and specific capacitance of the $MnFe_2O_4$ thin-film electrodes deposited at different deposition temperatures.



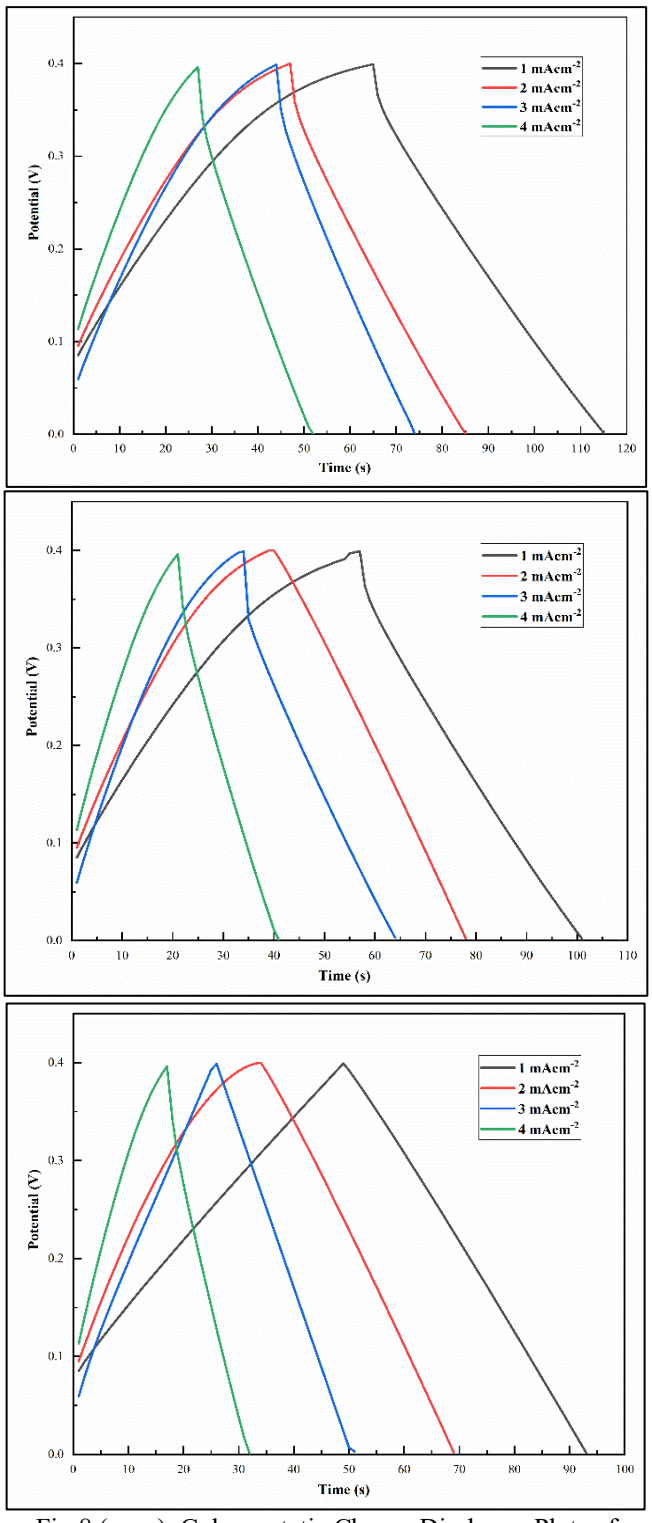


Fig 8 (a – e). Galvanostatic Charge-Discharge Plots of $MnFe_2O_4$ thin Films Prepared by Spray Pyrolysis at Various Deposition Temperatures: (a) 325ºC, (b) 350ºC, (c) 375ºC, (d) 400ºC, and (e) 425ºC, Respectively.

The corresponding GCD curves are shown in Fig. 8(a–e). The values of specific capacitance (SC) were calculated using the following formula [6]:

$$SC = \frac{I * \Delta t}{\Delta V * m} \quad (9)$$

ISSN No:-2456-2165 https://doi.org/10.38124/ijisrt/26nov1141

Where I denotes the constant discharge current, Δt represents discharge time, ΔV is the discharge voltage window, and m is the mass of the active electrode material.

For all the $MnFe_2O_4$ electrodes, the specific capacitance decreases with increasing current density. This behaviour can be attributed to the reduced accessibility of electrochemically active sites at higher current densities, where the available time for electrolyte-ion diffusion and faradaic reactions is limited.

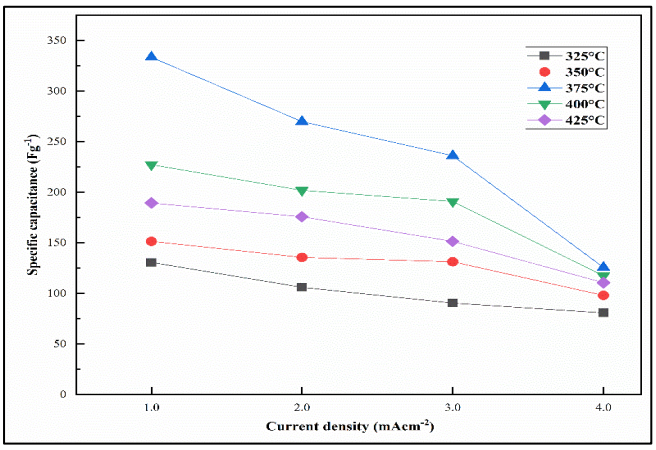


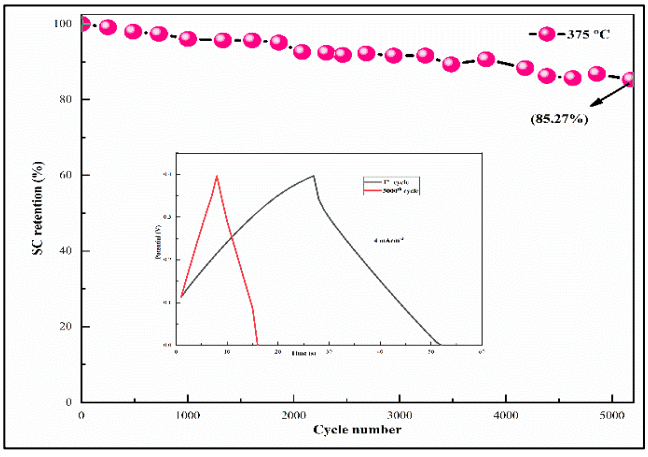
Fig 9 Variation of Specific Capacitance Values at Different Current Densities of $MnFe_2O_4$ thin Films Prepared by Spray Pyrolysis at Various Deposition Temperatures.

Figure 9 shows the plot of the variation of specific capacitance values of $MnFe_2O_4$ thin films with current densities (1 mA cm^{-2} to 4 mA cm^{-2}) at different deposition temperatures. Table 5 lists the specific capacitance values of $MnFe_2O_4$ thin films obtained by varying deposition temperature. The maximum specific capacitance of 333.48 F g^{-1} was recorded at the current density of 1 mA cm^{-2} for manganese ferrite thin films spray pyrolysed at 375ºC. The specific capacitance subsequently decreases for the films deposited at 400 and 425 °C. The enhanced charge-storage performance at 375 °C is consistent with the larger CV enclosed area and the relatively larger crystallite size observed from XRD, suggesting favourable electrochemical utilisation of the electrode at this deposition temperature. For comparison, Zate et al. reported a specific capacitance of 293.5 F g^{-1} at 1 mA cm^{-2} for $MnFe_2O_4$ thin films deposited by spray pyrolysis [18], which is quite lower than the value obtained in this study.

Table 5 Specific Capacitance Values of $MnFe_2O_4$ thin Films at Different Deposition Temperatures.

Current Density (mA cm^{-2})	Specific capacitance (F g^{-1})				
1	130.68	151.58	333.48	227.37	189.48
2	106.11	135.70	270	202.05	175.91
3	90.47	131.33	236.22	190.99	151.54
4	80.82	98.11	125.78	117.5	110.68

The cycling performance of 5000 cycles for $MnFe_2O_4$ thin films deposited at 375 °C at a current density of 4mA cm^{-2} is shown in Figure 10a. The inset graph shown in Figure 10a portrays charge-discharge curves for the first and five thousandth cycles. It was observed that the $MnFe_2O_4$ thin film synthesised at 375 °C shows 85.27% retention of its specific capacitance after 5000 continuous cycles at a current density of 4mA cm^{-2}.



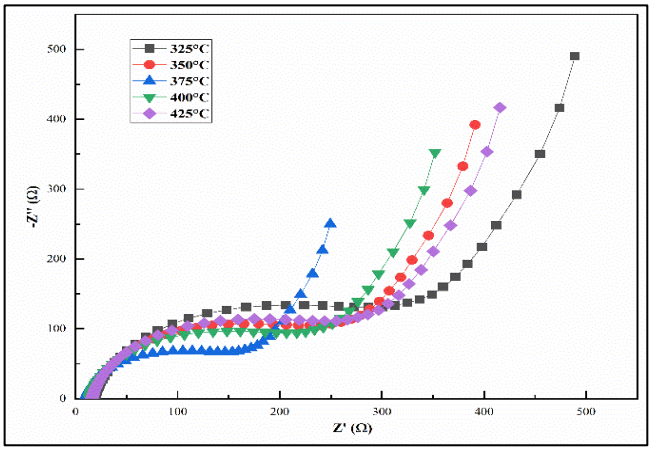


Fig 10a. Capacitive Retention Plot of $MnFe_2O_4$ thin Film Electrode at 375 °C Deposition Temperature; 10b. The Nyquist Plot of $MnFe_2O_4$ thin Films at Various Deposition Temperatures

- *Electrochemical Impedance Spectroscopy*

EIS was used to study the frequency response of $MnFe_2O_4$ thin films. Figure 10b shows the Nyquist spectrum of the $MnFe_2O_4$ thin films recorded over the frequency range

ISSN No:-2456-2165 https://doi.org/10.38124/ijisrt/26nov1141

of 1 Hz to 100 kHz with an AC signal amplitude of 5 mV. The intercept at the high-frequency region on the real axis, Z', is the equivalent series resistance (R_s), while the diameter of the semicircular response is associated with the charge-transfer resistance (R_{ct}) across the electrode-electrolyte interface. The R_s and R_{ct} values obtained from the Nyquist plots for $MnFe_2O_4$ thin film electrodes made by spray pyrolysis at different deposition temperatures are listed in Table 6. Both R_s and R_{ct} decrease with increasing deposition temperature up to 375 °C, reaching minimum values of 9.456 Ω and 170.6 Ω, respectively. Above 375 °C, both R_s and R_{ct} increase, indicating increased resistance to charge transport. The lower resistance values at 375 °C indicate reduced ohmic resistance and improved charge-transfer kinetics at the electrode–electrolyte interface, consistent with the enhanced electrochemical performance observed from the CV and GCD measurements.

Table 6 Nyquist Data of $MnFe_2O_4$ thin Films Prepared at Different Deposition Temperatures

Deposition temperature (°C)	R_s (Ω)	R_{ct} (Ω)
325	18.53	334.9
350	14.84	267.2
375	9.456	170.6
400	13.34	240.8
425	15.76	284.7

IV. CONCLUSION

The present study signifies that the deposition temperature plays a crucial role in determining the structural, optical, morphological, compositional, electrical, as well as electrochemical properties of $MnFe_2O_4$ thin films prepared via the spray pyrolysis method. Among the deposition temperatures examined, 375 °C was provided the most favourable overall properties under the present experimental conditions, including improved crystallinity, a cubic spinel structure, and a crystallite size of 36.32 nm. The optical band gap reached its minimum value of 2.68 eV at this temperature. FESEM analysis revealed a continuous granular morphology with relatively uniform surface coverage. EDAX analysis confirmed the presence of Mn, Fe and O in the deposited films, with the Mn-to-Fe atomic ratio being reasonably close to the nominal composition of MFO. The electrical resistivity measurements confirmed that the films are semiconducting in nature. $MnFe_2O_4$ thin film prepared at 375 ºC exhibited the highest specific capacitance of 333.48 F g^{-1} at a current density of 1 mA $cm^{-2}$and retained 85.27% of its initial specific capacitance after 5000 charge-discharge cycles at a current density of 4mA cm^{-2}, implying good cycling stability. EIS results indicated favourable charge-transfer characteristics of $MnFe_2O_4$, with a series resistance of 9.456 Ω and a charge-transfer resistance of approximately 170.6 Ω at 375 °C. These findings highlight the importance of deposition-temperature control in tuning the properties of $MnFe_2O_4$ thin films for electrochemical energy-storage applications.

➢ *Author Contributions:*

All authors contributed to the study conception and design. Material preparation, data collection and analysis were performed by all authors. The first draft of the manuscript was written by VBZ and RUS, and RVS commented on previous versions of the manuscript. All authors read and approved the final manuscript.

➢ *Funding:*

The authors would like to thank and acknowledge the Chhatrapati Shahu Maharaj Research Training and Human Development Institute (SARTHI), Pune, Government of Maharashtra, India, for funding support (sanction number: 2022/2022–23/2341).

➢ *Data Availability:*

No data was used for the research described in the article.

➢ *Declarations:*

Competing interests: The authors declare no competing interests.

REFERENCES

[1.] M. I. A. Abdel Maksoud et al., "Advanced materials and technologies for supercapacitors used in energy conversion and storage: a review," Environ. Chem. Lett., vol. 19, no. 1, pp. 375–439, Feb. 2021, doi: 10.1007/s10311-020-01075-w.

[2.] C. Zhong, Y. Deng, W. Hu, J. Qiao, L. Zhang, and J. Zhang, "A review of electrolyte materials and compositions for electrochemical supercapacitors," Chem. Soc. Rev., vol. 44, no. 21, pp. 7484–7539, Nov. 2015, doi: 10.1039/c5cs00303b.

[3.] A. K. Samantara and S. Ratha, Materials Development for Active/Passive Components of a Supercapacitor Background, Present Status and Future Perspective. Springer, 2018. doi: 10.1007/978-981-10-7263-5.

[4.] M. A. Scibioh and B. Viswanathan, "Supercapacitors: prospects and future direction," in Materials for Supercapacitor Applications, Elsevier, 2020, pp. 373–380. doi: 10.1016/b978-0-12-819858-2.00006-8.

[5.] S. Huang, X. Zhu, S. Sarkar, and Y. Zhao, "Challenges and opportunities for supercapacitors," APL Mater., vol. 7, no. 10, Oct. 2019, doi: 10.1063/1.5116146.

[6.] Z. Wu, Y. Zhu, X. Ji, and C. E. Banks, "Transition Metal Oxides as Supercapacitor Materials," in Nanomaterials in Advanced Batteries and Supercapacitors, Springer, 2016, pp. 317–344. doi: 10.1007/978-3-319-26082-2_9.

[7.] M. L. Aparna, A. N. Grace, P. Sathyanarayanan, and N. K. Sahu, "A comparative study on the supercapacitive behaviour of solvothermally prepared metal ferrite (MFe2O4, M = Fe, Co, Ni, Mn, Cu, Zn)

ISSN No:-2456-2165 https://doi.org/10.38124/ijisrt/26nov1141

nanoassemblies," J. Alloys Compd., vol. 745, pp. 385–395, May 2018, doi: 10.1016/j.jallcom.2018.02.127.

[8.] R. Rajalakshmi, K. P. Remya, C. Viswanathan, and N. Ponpandian, "Enhanced electrochemical activities of morphologically tuned MnFe2O4nanoneedles and nanoparticles integrated on reduced graphene oxide for highly efficient supercapacitor electrodes," Nanoscale Adv., vol. 3, no. 10, pp. 2887–2901, May 2021, doi: 10.1039/d1na00144b.

[9.] Z. Yu, L. Tetard, L. Zhai, and J. Thomas, "Supercapacitor electrode materials: Nanostructures from 0 to 3 dimensions," Energy Environ. Sci., vol. 8, no. 3, pp. 702–730, Mar. 2015, doi: 10.1039/c4ee03229b.

[10.] K. Dissanayake and D. Kularatna-Abeywardana, "A review of supercapacitors: Materials, technology, challenges, and renewable energy applications," J. Energy Storage, vol. 96, Aug. 2024, doi: 10.1016/j.est.2024.112563.

[11.] S. F. Shaikh, M. Ubaidullah, R. S. Mane, and A. M. Al-Enizi, "Types, Synthesis methods and applications of ferrites," in Spinel Ferrite Nanostructures for Energy Storage Devices, Elsevier, 2020, pp. 51–82. doi: 10.1016/B978-0-12-819237-5.00004-3.

[12.] M. S. Halper and J. C. Ellenbogen, "Supercapacitors: A Brief Overview," 2006. [Online]. Available: http://www.mitre.org/tech/nanotech

[13.] Z. S. Iro, C. Subramani, and S. S. Dash, "A brief review on electrode materials for supercapacitor," Int. J. Electrochem. Sci., vol. 11, no. 12, pp. 10628–10643, 2016, doi: 10.20964/2016.12.50.

[14.] H. Gao, J. Xiang, and Y. Cao, "Hierarchically porous CoFe2O4 nanosheets supported on Ni foam with excellent electrochemical properties for asymmetric supercapacitors," Appl. Surf. Sci., vol. 413, pp. 351–359, Aug. 2017, doi: 10.1016/j.apsusc.2017.04.067.

[15.] A. Soam, "Application of Ferrites as Electrodes for Supercapacitor," in Ferrites - Synthesis and Applications, IntechOpen, 2021. doi: http://dx.doi.org/10.5772/intechopen.99381.

[16.] T. Dippong, E. A. Levei, and O. Cadar, "Formation, structure and magnetic properties of MFe2O4 @SiO2 (M = Co, Mn, Zn, Ni, Cu) nanocomposites," Materials, vol. 14, no. 5, pp. 1–15, Mar. 2021, doi: 10.3390/ma14051139.

[17.] M. Goodarz Naseri, E. B. Saion, and A. Kamali, "An Overview on Nanocrystalline ZnFe2O4, MnFe2O4, and CoFe2O4 Synthesized by a Thermal Treatment Method," ISRN Nanotechnol., vol. 2012, pp. 1–11, Jul. 2012, doi: 10.5402/2012/604241.

[18.] M. K. Zate et al., "Structural, morphological and electrochemical supercapacitive properties of sprayed manganese ferrite thin film electrode," J. Anal. Appl. Pyrolysis, vol. 122, pp. 224–229, Nov. 2016, doi: 10.1016/j.jaap.2016.09.020.

[19.] R. P. Bhosale et al., "Morphology modulation of MnFe2O4 thin film electrode for enhanced performance of hybrid supercapacitor," J. Energy Storage, vol. 86, May 2024, doi: 10.1016/j.est.2024.111146.

[20.] A. Giribaldi et al., "Effect of the deposition temperature on the properties of MnFe2O4 thin films," J. Alloys Compd., vol. 1074, Jun. 2026, doi: 10.1016/j.jallcom.2026.189111.

[21.] P. S. Patil, "Versatility of chemical spray pyrolysis technique," Mater. Chem. Phys., vol. 59, no. 3, pp. 185–198, 1999, doi: 10.1016/S0254-0584(99)00049-8.

[22.] D. Perednis and L. J. Gauckler, "Thin Film Deposition Using Spray Pyrolysis," J. Electroceramics, vol. 14, pp. 103–111, 2005, doi: 10.1007/s10832-005-0870-x.

[23.] V. A. Jundale and A. A. Yadav, "Electrochemical properties of CoFe2O4 thin film electrodes prepared by spray pyrolysis," Thin Solid Films, vol. 772, May 2023, doi: 10.1016/j.tsf.2023.139821.

[24.] V. D. Patil et al., "Spinel nickel ferrite (NiFe2O4) materials synthesized via spray-pyrolysis for electrochemical supercapacitor application," Discov. Electrochem., vol. 1, no. 1, Aug. 2024, doi: 10.1007/s44373-024-00003-9.

[25.] V. A. Jundale, D. A. Patil, and A. A. Yadav, "Preparation and characterization of NiFe2O4 thin films for supercapacitor applications," Phase Transit., vol. 95, no. 11, pp. 786–802, 2022, doi: 10.1080/01411594.2022.2122825.

[26.] V. S. Kumbhar, A. D. Jagadale, N. M. Shinde, and C. D. Lokhande, "Chemical synthesis of spinel cobalt ferrite (CoFe2O4) nano-flakes for supercapacitor application," Appl. Surf. Sci., vol. 259, pp. 39–43, Oct. 2012, doi: 10.1016/j.apsusc.2012.06.034.

[27.] V. Nagarajan and A. Thayumanavan, "Spray deposited MnFe2O4 thin films for detection of ethanol and acetone vapors," Appl. Surf. Sci., vol. 428, pp. 748–756, Jan. 2018, doi: 10.1016/j.apsusc.2017.09.156.

[28.] R. A. Reddy et al., "Structural, electrical and magnetic properties of cobalt ferrite with Nd3+ doping," Rare Met., vol. 41, no. 1, pp. 240–245, Jan. 2022, doi: 10.1007/s12598-019-01285-4.

[29.] M. M. N. Ansari, S. Khan, R. Bhargava, and N. Ahmad, "An extensive study of electrical properties of MnFe2O4 nano-ferrite," in AIP Conference Proceedings, American Institute of Physics Inc., Jul. 2019. doi: 10.1063/1.5112915.

[30.] T. T. N. Nha et al., "Microwave-assisted co-precipitation synthesis of MFe2O4 nanoferrites (M = Co and Mn) using biogenic coir extract and their physical characterization," RSC Adv., vol. 15, no. 36, pp. 29571–29592, Aug. 2025, doi: 10.1039/d5ra04897d.

[31.] T. D. Thanh et al., "Structural, optical, magnetic properties and energy-band structure of MFe2O4 (M = Co, Fe, Mn) nanoferrites prepared by co-precipitation technique," RSC Adv., vol. 14, no. 33, pp. 23645–23660, Jul. 2024, doi: 10.1039/d4ra04692g.

[32.] K. Chand Verma, V. Pratap Singh, M. Ram, J. Shah, and R. K. Kotnala, "Structural, microstructural and magnetic properties of NiFe2O4, CoFe2O4 and MnFe2O4 nanoferrite thin films," J. Magn. Magn. Mater., vol. 323, no. 24, pp. 3271–3275, Dec. 2011, doi: 10.1016/j.jmmm.2011.07.029.

ISSN No:-2456-2165 https://doi.org/10.38124/ijisrt/26nov1141

[33.] J. L. Gunjakar, A. M. More, V. R. Shinde, and C. D. Lokhande, “Synthesis of nanocrystalline nickel ferrite (NiFe2O4) thin films using low temperature modified chemical method,” J. Alloys Compd., vol. 465, no. 1–2, pp. 468–473, Oct. 2008, doi: 10.1016/j.jallcom.2007.10.130.

[34.] A. R. Chavan, J. S. Kounsalye, R. R. Chilwar, S. B. Kale, and K. M. Jadhav, “Cu2+substituted NiFe2O4 thin films via spray pyrolysis technique and their high-frequency devices application,” J. Alloys Compd., vol. 769, pp. 1132–1145, Nov. 2018, doi: 10.1016/j.jallcom.2018.08.061.